Reciprocity between the effects of resonant scattering and enhanced radiated power by electrically small antennas in the presence of nested metamaterial shells

Richard W. Ziolkowski* and Allison D. Kipple†
Department of Electrical and Computer Engineering, The University of Arizona, 1230 E. Speedway Boulevard, Tucson, Arizona 85721-0104, USA

(Received 11 July 2004; revised manuscript received 8 April 2005; published 7 September 2005)

Reciprocity between the power scattered by nested metamaterial shells and the power radiated by an antenna centered within those nested shells has been investigated. Resonant scattering caused by an incident, fundamental transverse-magnetic mode was found to be reciprocal to the power resonantly radiated by an electrically small electric dipole for a variety of configurations. These findings indicate that the power radiated by an electrically small antenna and scattered by an electrically small object can be significantly increased through the use of realizable metamaterials.

DOI: 10.1103/PhysRevE.72.036602 PACS number(s): 41.20.−q, 84.40.Ba, 42.25.Fx

Consider an electrically small electric dipole of length ℓ that is driven by the current I_0 at the frequency f_0 corresponding to the wavelength $\lambda = 1/(f_0\sqrt{|\varepsilon|\,|\mu|})$ and that is embedded in a double-positive (DPS) medium, where the permittivity $\varepsilon > 0$ and the permeability $\mu > 0$ so that the wave number $k = \omega\sqrt{\varepsilon}\sqrt{\mu} > 0$ and the wave impedance $\eta = \sqrt{\mu}/\sqrt{\varepsilon} > 0$. It produces the complex power at the radius r given by [1]

$$P = \oiint_S \left(\frac{1}{2}\vec{E}_\omega \times \vec{H}^*_\omega\right)\cdot \hat{r}\, dS = \eta\left(\frac{\pi}{3}\right)\left|\frac{I_0\ell}{\lambda}\right|^2\left[1 - j\frac{1}{(kr)^3}\right]$$

$$= P_{rad} + jP_{reac} \tag{1}$$

[using the engineering convention for time-harmonic signals: $\exp(+j\omega t)$]. The (well-known) capacitive reactive power component in Eq. (1) is very large near the antenna and severely limits its efficiency as a radiator, i.e., the reactance ratio $P_{reac}/P_{rad} \gg 1$ for $kr \ll 1$ indicating that the radiated power is much smaller than the reactive power for electrically small radiators. The dipole's reactive power is dominated by the electric field energy, i.e., $P_{reac} = \omega(W_m - W_e)$ where W_e and W_m are the corresponding time averaged electric and magnetic field energies. This work was instigated when we noticed that this capacitive reactance becomes an inductive reactance when the same antenna is embedded in a double-negative (DNG) medium, i.e., in a medium whose permittivity and permeability are negative, $\varepsilon < 0$ and $\mu < 0$ so that the wave number $k = \omega\sqrt{\varepsilon}\sqrt{\mu} = -\omega\sqrt{|\varepsilon|}\sqrt{|\mu|} < 0$ while the wave impedance $\eta = \sqrt{\mu}/\sqrt{\varepsilon} = \sqrt{|\mu|}/\sqrt{|\varepsilon|} > 0$ [2]. Basically, the negative permittivity loading the capacitor makes it act as an inductor. This behavior suggested a possible means of resonantly matching these capacitive and inductive behaviors. Consequently, we have investigated the possibility of naturally matching an electrically small electric dipole antenna to free space by surrounding it with a hollow DNG shell.

We have demonstrated with analytical and numerical investigations [3] that the capacitance exhibited by an electrically small electric dipole in free space can be matched by the inductance of a surrounding lossless DNG shell, creating an effective LC resonator configuration which significantly increases the real power radiated by the dipole with a corresponding decrease in the total reactance ratio. In particular, the three-region (two nested sphere) geometry used in the majority of our investigations is shown in Fig. 1. The dipole is located along the vertical z axis in the center of the nested spheres. Relations for the electric and magnetic vector potentials, and for the resulting electric and magnetic fields, were obtained in a straightforward manner for each region. The unknown coefficients in those relations were found by applying the appropriate electromagnetic boundary conditions, that is, by making the tangential fields, E_θ and H_ϕ, continuous across each shell interface. The resulting equations, presented in our previous work [3], were straightforward to ob-

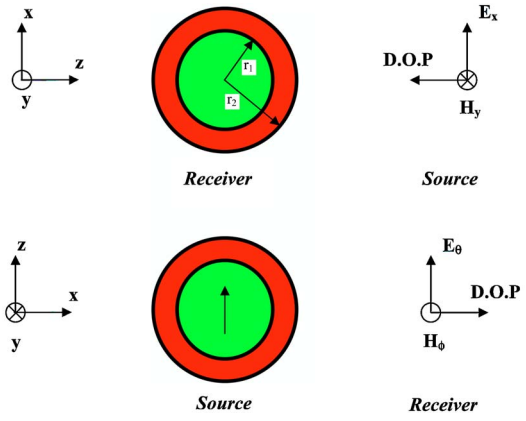

FIG. 1. (Color online) The three-region (two nested sphere) geometries used to investigate the reciprocity of the scattering (upper) and source (lower) problems. For both cases, region 1 is given by ε_1, μ_1 for $r \leq r_1$; region 2 has ε_2, μ_2 for $r_1 < r \leq r_2$; and region 3 has ε_3, μ_3 for $r_2 < r$. The direction of propagation (D.O.P.) of the wave leaving the source and incident on the receiver is shown.

*Email address: ziolkowski@ece.arizona.edu
†Present address: Electronic Proving Ground, Fort Huachuca, AZ 85613. Email address: allison.kipple@epg.army.mil

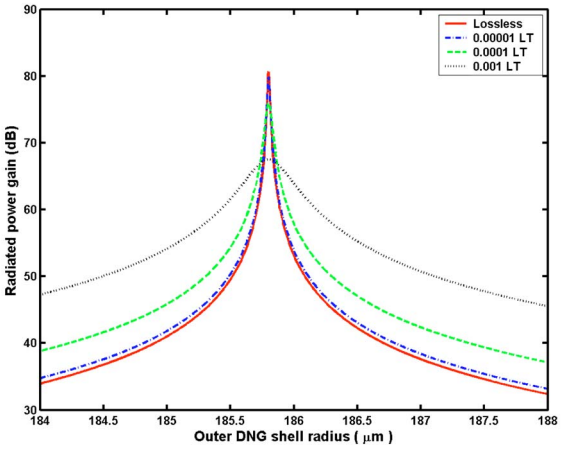

FIG. 2. (Color online) The radiated power gain for an electrically small electric dipole antenna located at the center of various lossless and lossy DNG shells with inner radius $r_1=100$ μm.

tain and solve numerically. They were generalized here to include passive losses in the medium parameters, i.e., we let $\varepsilon=\varepsilon_r\varepsilon_0-j\varepsilon''$ and $\mu=\mu_r\mu_0-j\mu''$ where $\varepsilon_r,\mu_r<0$ and $\varepsilon'',\mu''>0$. We embedded an electrically small dipole $\ell=100$ μm $=\lambda_0/300$ driven at $f_0=10$ GHz (free space wavelength $\lambda_0=3.0$ cm) in a small sphere of free space (DPS) material with a radius of $r_1=100$ μm, which in turn was surrounded by a DNG shell of outer radius r_2 with the permittivity and permeability values: $(\varepsilon_{2r},\mu_{2r})=(-3,-3)$, and equal electric and magnetic loss tangents, $LT=\varepsilon''/|\varepsilon_r|\varepsilon_0=\mu''/|\mu_r|\mu_0$, set to the fixed values $LT=0$, 0.00001, 0.0001, and 0.001. The external region, $r>r_2$, was assumed to be free space.

The radiated power gain was obtained, i.e., the ratio

$$RP_{gain}=P_{rad,\text{with shell}}/P_{rad,\text{without shell}}, \tag{2}$$

where the power radiated by the $\ell=100$ μm dipole in the presence of the DNG shell system, $P_{rad,\text{with shell}}$, was normalized by the power radiated by a reference dipole in free space, $P_{rad,\text{without shell}}$, whose length ℓ_{ref} is equal to the diameter of the outer sphere of the DNG shell that produces the maximum radiated power. Because the dipole antennas in both cases were ideal, the same 1.0 A driving current was assumed in both cases. These radiated power gain results are plotted as a function of the DNG shell's outer radius in Fig. 2. As reported previously, the maximum in the lossless case occurs at $r_{2,\max}=185.8$ μm and, hence, $\ell_{ref}=371.6$ μm $\approx\lambda_0/81$. The fact that the optimum configuration produces a resonant enhancement of the power radiated despite the fact that it is much smaller than a free space wavelength ($r_{2,\max}\approx\lambda_0/161$) is surprising. It occurs because the electrically small elements, the dipole, and the DNG shell, form a naturally resonant system. The occurrence of this natural mode was confirmed mathematically by demonstrating that the determinant of the solution system approaches zero for these material and geometry parameters. Because the enhanced radiated power gain occurs when the dipole and DNG shell interactions are resonant, the losses simply reduce the peak of the response and cause a broadening of the resonance region. They do not make the effect disappear. The contour plot of the magnitude of the real part of the magnetic field distribution for the DNG shell with $r_1=100$ μm and $r_2=185.8$ μm given in Fig. 3 illustrates the natural mode that is excited by the dipole.

As shown in [4], an electrically small dipole radiating into free space can be described by a classic C-L transmission line (terminated with the free space impedance) that acts as a high pass filter. As a result, it is poorly matched to free space yielding little radiated power while creating a large reactive near field. In essence, the dipole field sheds most of its power in its near field region as it tunnels through a large potential barrier. As shown in [3], the DNG shell introduces a dual L-C transmission line, i.e., a low pass filter, which can be resonantly matched to the original line. The DNG shell significantly reduces the potential barrier allowing a resonant coupling of the power into the far field.

The very small radiation resistance of the free space infinitesimal dipole is well-known from Eq. (1) and is $R_{\text{rad,free space}}=2\eta(\pi/3)|\ell/\lambda_0|^2\approx 80\pi^2|\ell/\lambda_0|^2=0.0088$ Ω for the DNG shell case. It is a common descriptor of the poor radiated power characteristics of such an electrically small dipole in free space. Because the dipole in the DNG shell and the reference free space dipole are both treated as ideal and both are driven with the same current value, the resonant radiated power gain observed in Fig. 2 is equivalent to the resonant increase in the effective radiation resistance of the dipole-DNG shell system. On the other hand, the ideal nature of these dipoles also means that their corresponding radiation efficiencies, i.e., the ratio of the power radiated to the power input from a real source, cannot be calculated with their analytical models. Recent numerical studies with commercial software that includes the circuit elements used to drive a realistic dipole antenna and, hence, its input and accepted powers, have been performed to calculate the power radiated by a dipole-DNG shell system and by the same dipole in free space and will be reported elsewhere. They show, as suggested by the results given here, that an electrically small dipole-DNG shell system can be designed to be resonant and matched to a power source and thus produce a resonant increase in the radiation efficiency over that of the antenna alone in free space.

Recent work by Alú and Engheta has shown a direct correlation between the behavior of nested DPS-DNG and nested epsilon-negative (ENG)-mu-negative (MNG) systems [5] and has additionally demonstrated resonant scattering from nested metamaterial shells [6], including various combinations of DPS, DNG, ENG, and MNG shells. Their findings led us to investigate the possibility of reciprocity between the radiation and scattering resonances for a variety of nested metamaterial shells. Should reciprocity be observed, we then hypothesized that the single-negative (SNG) nested sphere geometries, composed of various combinations of ENG and MNG metamaterial shells and found to support these lowest order transverse-magnetic (TM) (dipole) scattering resonances, would also maximize the power radiated by an electrically small electric dipole. We thus anticipated that the electrically small electric dipole could be matched with a nested set of MNG-ENG shells—or even a single ENG

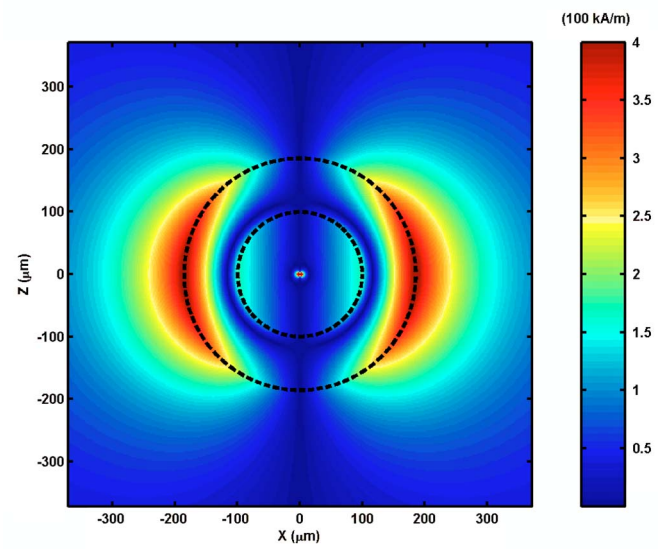

FIG. 3. (Color online) Contour plot of the magnitude of the real part of the magnetic field distribution produced by the resonant electric dipole—lossless DNG shell system.

shell—in place of the DNG shell used previously. The possibility of matching an electrically small antenna with an ENG material alone is especially appealing, since ENG media are found in nature (e.g., cold electron plasmas and other Drude systems) and have been manufactured artificially for many years, e.g., the bed-of-nails or wire medium [7].

The reciprocal scattering problem is also shown in Fig. 1. The source and receiver have been interchanged. A plane wave polarized along the x direction is incident from infinity along the $-z$ axis onto the nested two-sphere configuration. However, because the nested spheres are electrically small, only the transverse magnetic with respect to the r direction $\mathrm{TM}_r(n=1,m=1)$ mode (mode number n for the polar angle θ, m for the azimuthal angle ϕ) of this plane wave causes any significant response and was used in the calculations below. The scattering can thus be viewed in terms of an induced dipole oriented along the x axis and centered at the origin. This mode also provided the best standard analytical match to the above z-oriented electrically small electric dipole analysis, which corresponds to radiation of the $\mathrm{TM}_r(n=1,m=0)$ mode. The nested spheres in the scattering case are treated as the receiver, the received signal being represented by the energy captured by the interior DPS sphere. From reciprocity one would expect that there will be a large scattered field only if the energy captured by the nested spheres resonantly drives the induced dipole.

The electric and magnetic field relations for the three-region scattering geometry and the corresponding derived scattering parameters were obtained and calculated. The simulator was validated using well-known cases, including dielectric Mie scattering from each shell interface with a DPS interior; its output was also compared to data provided by Alú and Engheta [8]. The DPS-DNG systems were then analyzed numerically for scattering resonances.

The energy received and stored in the inner DPS sphere as a result of an incident 10 GHz $\mathrm{TM}_r(n=1,m=1)$ wave scattering from the lossless nested DPS-DNG $r_1=100$ μm configuration used in the source problem is shown in Fig. 4, plotted as a function of the DNG shell's outer radius. The energy stored in the inner free space (DPS) sphere when it is surrounded by the DNG shell is normalized relative to the energy that would be stored in a free space sphere whose radius equals the outer radius of the resonant DNG shell, $r_{2,\max}$. The peak in the normalized stored energy for the $(\varepsilon_2,\mu_2)=(-3.0\varepsilon_0,-3.0\mu_0)$ case occurs at $r_{2,\max}=185.8$ μm $\approx\lambda_0/161$, the same radius at which the source problem radiated power gain was maximized. The determinant of the $\mathrm{TM}_r(n=1,m=1)$ scattering coefficient matrix produces a sharp minimum at this radius, indicating the presence of a natural mode. The ratio $r_{2,\max}/r_1$ agrees with the value predicted by the resonant scattering expression given in [6], obtained from a quasistatic ($kr_i\ll 1$, $i=1,2$) approximation of the scattering matrices. When considering the energy stored in the real and imaginary components of the electric and magnetic fields within the inner sphere, it was found that the energy stored in the real part of the magnetic field goes to a local maximum while the energy stored in the real part of the electric field goes to local minimum for the resonant geometry. Put another way, the magnetic fields in the DPS-DNG scattering system become completely real at the resonant configuration, while the electric fields become completely imaginary. The same behavior is exhibited in the DNG shell. This indicates that the resonant DPS-DNG system is behaving as a TM resonator with matched capacitance and inductance. The magnitude of the real part of the magnetic field distribution generated for this case is shown in Fig. 5. Clearly, the same natural mode of the nested sphere system found in the source problem was excited in the scattering problem. Reciprocity of the source and scattering problems in the presence of the DNG shell is thus established.

To further emphasize this reciprocity, the total scattering cross section data for the $\mathrm{TM}_r(n=1,m=1)$ excitation

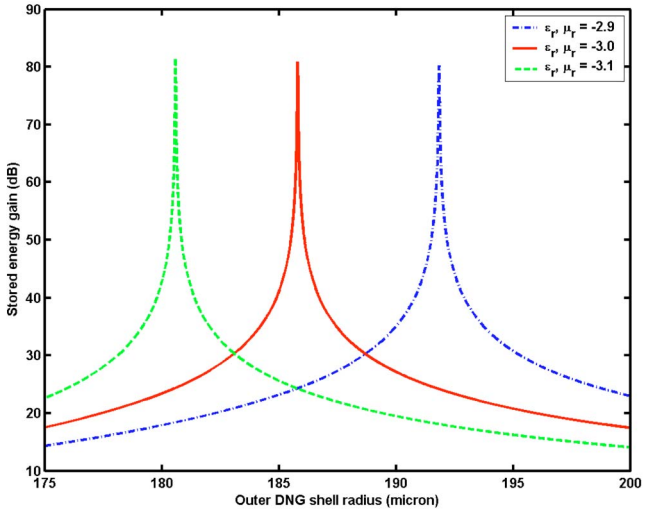

FIG. 4. (Color online) The gain of the energy stored in the inner sphere when the $\mathrm{TM}_r(n=1,m=1)$ mode scatters from various lossless DNG shells with inner radius $r_1=100$ μm.

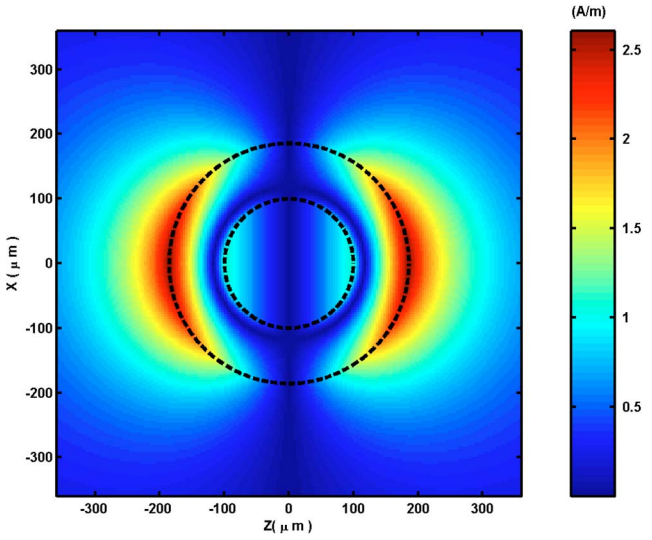

FIG. 5. (Color online) Contour plot of the magnitude of the real part of the magnetic field distribution produced when the $\mathrm{TM}_r(n=1,m=1)$ mode is scattered from the resonant lossless DNG shell system.

$$\sigma_{Total} = \frac{2\pi}{k_0^2}\sum_{n=1}^{\infty}(2n+1)\left[\left|c_n^{\mathrm{TM}}\right|^2 + \left|c_n^{\mathrm{TE}}\right|^2\right] \approx 3\frac{2\pi}{k_0^2}\left|c_1^{\mathrm{TM}}\right|^2 \tag{3}$$

normalized to the unity cross section for this exciting mode (i.e., to the total scattering cross section with the scattering coefficient being one, $\sigma_{unity}=6\pi/k_0^2=3\lambda_0^2/2\pi$, which is equal to the resonant short circuit scattering cross section of a very short dipole antenna [9]) is given in Fig. 6. It also exhibits a resonant enhancement for the same geometry. In fact the dipole scattering coefficient goes to one at the critical radius, $r_{2,\max}\approx\lambda_0/161$, for the $(\varepsilon_2,\mu_2)=(-3.0\varepsilon_0,-3.0\mu_0)$ case, again despite the extremely small size of the scatterer. The

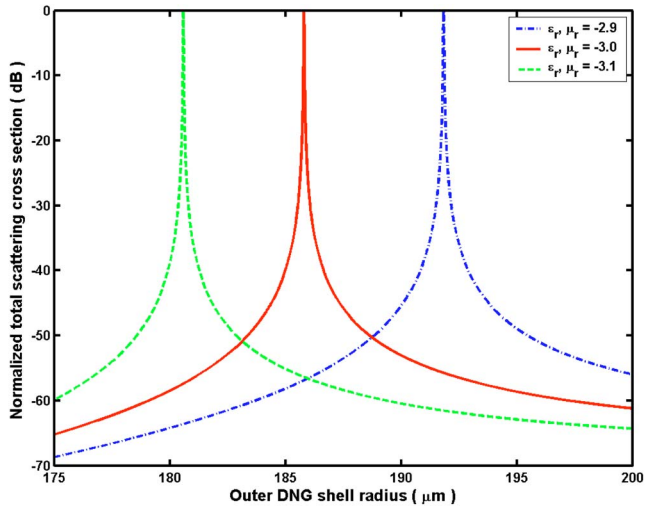

FIG. 6. (Color online) The normalized total scattering cross section when the $\mathrm{TM}_r(n=1,m=1)$ mode scatters from various lossless DNG shells with inner radius $r_1=100$ μm.

incident wave induces a dipole moment over the inner DPS sphere which then reradiates as an electrically small antenna. A resonant response results from the presence of the inductive DNG shell that matches this capacitive element to free space.

The (detector) energy and the total scattering cross section for the $r_1=100$ μm DNG shell configurations with $(\varepsilon_2,\mu_2)=(-2.9\varepsilon_0,-2.9\mu_0)$ and $(\varepsilon_2,\mu_2)=(-3.1\varepsilon_0,-3.1\mu_0)$ are also given, respectively, in Figs. 4 and 6 for comparison. The nested sphere configuration is resonant for a smaller outer shell radius when the index of refraction of the shell is more negative. Reciprocity between these and the corresponding dipole source results has been verified.

Along with the DPS-DNG analyses, source and scattering resonances were analyzed for a wide variety of DPS-SNG and MNG-ENG systems. They were also studied for related four region (three nested sphere) configurations, e.g., for a nested DPS-MNG-ENG configuration. For example, several source and scattering resonances for configurations with similar sizes and material parameters as the "supergain" case presented above were observed, including: (1) inner MNG sphere with $(\varepsilon_r,\mu_r)=(1,-1)$ and radius $r_1=100.0$ μm, and surrounding ENG shell with $(\varepsilon_r,\mu_r)=(-3,3)$ and $r_2=185.8$ μm; (2) inner DPS, free space sphere with radius $r_1=99.9$ μm, and surrounding ENG shell with $(\varepsilon_r,\mu_r)=(-3,1)$ and $r_2=185.8$ μm; and (3) an example four-region case with an inner DPS, free space sphere with radius $r_1=100.0$ μm, surrounding MNG shell with $(\varepsilon_r,\mu_r)=(1,-5)$ and $r_2=133.9$ μm, and outer ENG shell with $(\varepsilon_r,\mu_r)=(-5,1)$ and $r_3=185.8$ μm.

The DPS-ENG case is of particular interest due to the possibility of manufacturing a DPS-ENG system while still exploiting the resonance properties emphasized by the DPS-DNG source and scattering cases. In particular, the fact that the shell must be inductive to achieve a resonant match with an electrically small dipole antenna infers that an ENG shell should be adequate to achieve similar results, i.e., because the shell is electrically small, it will also respond as a small capacitive element but contain a negative permittivity and, hence, it will effectively act as an inductive element. With a dipole of length $\ell=100$ μm in free space surrounded by a lossless ENG shell with inner radius $r_1=100$ μm and material properties $(\varepsilon_r,\mu_r)=(-3.0,1)$, the radiated power gain as a function of the outer radius is shown in Fig. 7. The resonant peak occurs at $r_{2,\max}=185.9$ μm. The resonant behavior for lossless ENG shells with material properties $(\varepsilon_r,\mu_r)=(-2.9,1)$ and $(\varepsilon_r,\mu_r)=(-3.1,1)$ are also shown in Fig. 7 for comparison. The radiated power gain for all of these systems is comparable in magnitude to that of the dipole-lossless DNG shell case shown in Fig. 2. Plots of the electric and magnetic field distributions for the resonant dipole-ENG shell system show the same resonance behavior illustrated in Fig. 3.

Because a shell with a thickness of 85.9 μm would be very challenging to fabricate even with an ENG wire medium or some other currently known inductively loaded periodic metamaterial at 10 GHz, similar results have been considered at much lower frequencies. They indicate that an ENG shell may indeed provide a practical alternative to a

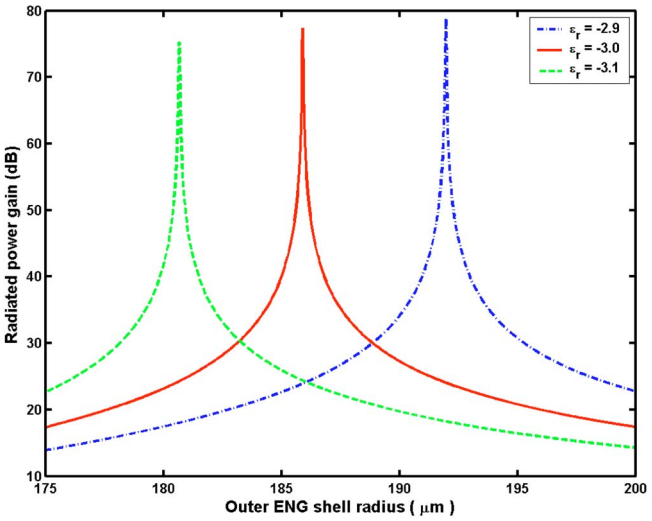

FIG. 7. (Color online) The radiated power gain for an electrically small electric dipole antenna located at the center of various lossless ENG shells with inner radius $r_1=100$ μm.

DNG shell for purposes of resonantly matching an electrically small TM_r-producing antenna to free space. Cases have also been considered to show similar enhancements for an electrically small loop antenna (magnetic dipole) surrounded by an MNG shell. Both the electric and magnetic dipole configurations may have potential sensor applications as well.

We note that past literature on antennas radiating in the presence of dielectric and plasma coatings further supports the results reported here. For instance, analyses of the behavior of dipole antennas surrounded by dielectric and plasma shells and centered in dielectric spheres were considered in [10–14]. Expressions in [14] for the fields radiated by an electrically small dipole in a dielectric sphere exhibit reciprocity with the well-known Rayleigh scattering results for electrically small dielectric spheres, particularly for an ENG medium having the permittivity $\varepsilon_r=-2$, as would occur with plasmonic resonances in the optical regime. A plasma coated hemispherical dipole was shown to have a radiated power enhancement in [15]. Experimental results showing enhanced radiated power from an electrically small antenna that is completely surrounded by a plasma of finite size and is driven at frequencies below the plasma frequency were reported in [16]. Scattering from nested spheres was reviewed in [17]; the backscattering cross-section expression for an ENG shell in the electrically small limit exhibits a resonance at a radius ratio that agrees approximately with the results given in [6] and here.

The resonant enhancement of the power radiated by an electrically small electric dipole when it is surrounded by a properly designed DNG shell was found to correlate with the scattering enhancements produced by the same DPS-DNG shell configuration. These resonant enhancements occurred even though the sizes of these configurations were very small compared to the radiation wavelength. Fundamental TM scattering resonances, which were observed for various nested MNG-ENG and DPS-ENG configurations, were additionally found to correlate with resonances in the radiated power produced by an electrically small electric dipole centered within those systems. The DPS-ENG results were of particular interest, due to the known possibility of manufacturing ENG materials. They produced radiated and scattered power gains of the same order of magnitude as the DNG-based systems. Future work will focus on developing an approach for determining the "best" DNG and ENG metamaterials to achieve the spherical shell configuration, given the specific material and size constraints. To demonstrate that metamaterial-based configurations can significantly increase an antenna's radiated power, experimental designs to realize the predicted resonant match between an electrically small TM_r-producing antenna, such as the dipole with all of its associated driving circuits, and an ENG shell, as well as between other types of antennas and the appropriate metamaterials, are currently under investigation.

This work was supported in part by DARPA under Contract No. MDA972-03-100 and by ONR under Contract No. 14-04-1-0320. The authors would like to thank Mr. Andrea Alú and Professor Nader Engheta for kindly sharing their results with us for the comparisons used in this paper.

[1] C. A. Balanis, *Antenna Theory Analysis and Design*, 2nd ed. (Wiley, New York, 1997).
[2] R. W. Ziolkowski and E. Heyman, Phys. Rev. E **64**, 056625 (2001).
[3] R. W. Ziolkowski and A. D. Kipple, IEEE Trans. Antennas Propag. **51**, 2626 (2003).
[4] L. J. Chu, J. Appl. Phys. **19**, 1163 (1948).
[5] A. Alú and N. Engheta, IEEE Trans. Antennas Propag. **51**, 2558 (2003).
[6] A. Alú and N. Engheta, J. Appl. Phys. **97**, 094310 (2005).
[7] W. Rotman, IRE Trans. Antennas Propag. **10**, 82 (1962).
[8] A. Alú and N. Engheta (private communication).
[9] J. D. Krauss, *Antennas*, 2nd ed. (McGraw-Hill, New York, 1988), pp. 31–44.
[10] H. R. Raemer, IRE Trans. Antennas Propag. **10**, 69 (1962).
[11] H. B. Keller and J. B. Keller, J. Appl. Phys. **20**, 393 (1949).
[12] M. G. Andreasen, IRE Trans. Antennas Propag. **5**, 337 (1957).
[13] R. V. Row, IEEE Trans. Antennas Propag. **12**, 646 (1964).
[14] J. Galejs, *Antennas in Inhomogeneous Media* (Pergamon, Oxford, 1969), Chap. 4.
[15] N. M. Roslyakov and N. A. Tenyakova, J. Commun. Technol. Electron. **49**, 1133 (2004).
[16] K. M. Chen and C. C. Lin, Proc. IEEE **56**, 1595 (1968).
[17] D. E. Burrick, in *Radar Cross Section Handbook*, edited by G. T. Ruck, D. E. Barrick, W. D. Stuart, and C. K. Krichbaum, (Plenum, New York, 1970), pp. 179–195.